ARCHIVES OF HYDROENGINEERING
Volume XL 1993 Number 3-4

*RYSZARD STAROSZCZYK**

Solution of Lamb's Steady-State Plane Problem for Biot's Medium by the Finite Element Method

Abstract

In the paper plane Lamb's problem for a two-phase medium is solved by the use of the finite element method. In order to reduce considerations to a finite domain artificial boundaries, consisting of viscous dashpots, are introduced. Discrete results obtained are compared with those evaluated analytically.

Key words: two-phase medium, half-space, wave propagation, finite element method

1. Introduction

In many dynamical structure-soil interaction problems encountered in practice we deal with open systems of a semi-infinite type. In such problems, energy is transmitted by progressive waves from the source of disturbances to infinity. In order to solve such problems, because of the geometrical features of the systems, we must usually resort to discrete methods. As the latter require the use of only a limited number of discrete points, it is necessary to reduce considerations to a finite area of the soil in the vicinity of

*R. STAROSZCZYK, Institute of Hydroengineering, Polish Academy of Sciences, ul. Kościerska 7, 80–953 Gdańsk, Poland.

the vibrating structure and to introduce imaginary boundaries enclosing the field of interest. At the boundaries appropriate conditions should be formulated so as to ensure an undisturbed flow of energy from the finite region to infinity. These conditions can be constructed in some ways. One of the possible approaches consists in the setting up of a system of viscous dashpots at the boundary to absorb energy of incoming waves. Such a method was proposed and successfully applied in solving a plane, steady-state wave propagation problem for a purely elastic half-space by Lysmer and Kuhlemeyer (1969). Satisfactory results were also obtained by Filipkowski and Sienkiewicz (1988), who applied this method for a case of viscoelastic solid. As regards a two-phase, fluid-saturated poroelastic medium, such absorbing conditions were proposed in the earlier paper of the author (Staroszczyk 1992a). At the viscous boundary three groups of infinitesimal dashpots oriented normally and tangentially to it are established. Their aim is to absorb three types of body waves (two dilatational and one shear) which propagate in the two-phase material. Parameters of the dashpots are so chosen as to ensure maximum absorbing ability of the viscous boundary. As the results of numerical analysis showed, the proposed boundary is able to absorb about 89 – 95 percent of the incoming wave energy, depending on the frequency of oscillations and the kind of soil (sandstone, coarse and fine sands were considered). In the paper mentioned the parameters of the viscous dashpots set up at a vertical boundary perfectly absorbing Rayleigh-type surface waves are also evaluated.

The purpose of the present paper is to examine the usability of the proposed approximate transmission boundary conditions for the two-phase media in solving steady-state plane problems, typical for engineering practice. To this aim, Lamb's problem which consists in the determination of displacement fields of the medium due to tractions applied at the free surface of the half-space, is investigated. The considerations are confined to oscillations which are small, linear and harmonic in time. The motion of the fluid-saturated poroelastic medium is studied on the basis of the dynamic theory of consolidation, formulated by Biot (1956). A solution to the problem is constructed by means of the finite element method. Employing the discrete model constructed, some numerical calculations have been made and their results are compared with those obtained analytically (Staroszczyk 1992b).

2. Formulation of the Problem

The problem under consideration is shown in Figure 1. A fluid-saturated poroelastic medium, which occupies the half-space $z \geq 0$, is subjected to the time harmonic tractions $q_{zz}(x)\exp(i\omega t)$, $q_s(x)\exp(i\omega t)$ and $q_{xz}(x)\exp(i\omega t)$ applied at the free boundary $z = 0$, with ω being the angular frequency of vibrations. The aim of the investigation is to determine displacement fields of the skeleton and the pore fluid due to exciting surface loads.

The equations governing the motion of the porous medium filled with a viscous fluid are taken as those formulated by Biot (1956). In the plane Oxz coordinate system

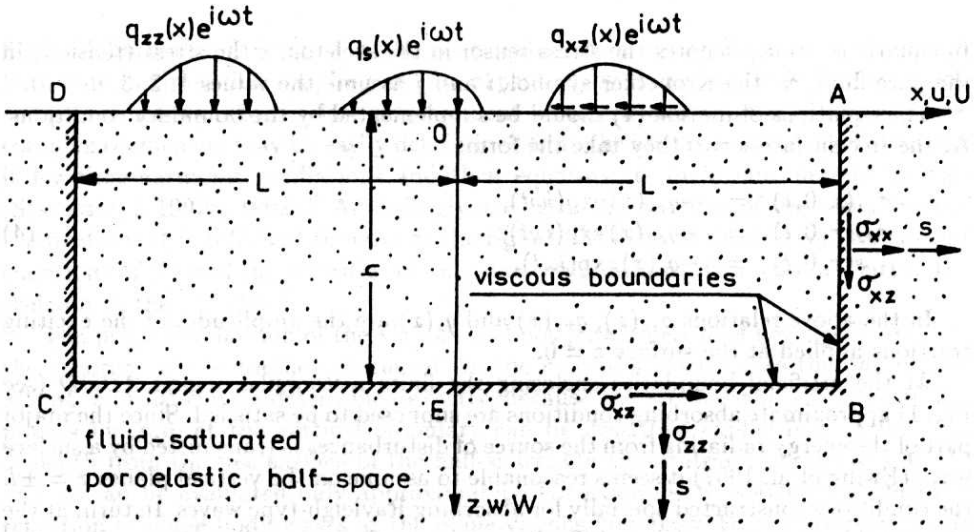

Fig. 1. Finite dynamical model of the Lamb's plane problem

they have the form:

$$\nabla^2(P\operatorname{div}\mathbf{u}+Q\operatorname{div}\mathbf{U}) = \frac{\partial^2}{\partial t^2}(\rho_{11}\operatorname{div}\mathbf{u}+\rho_{12}\operatorname{div}\mathbf{U})+\zeta\frac{\partial}{\partial t}\operatorname{div}(\mathbf{u}-\mathbf{U}), \quad (1)$$

$$\nabla^2(Q\operatorname{div}\mathbf{u}+R\operatorname{div}\mathbf{U}) = \frac{\partial^2}{\partial t^2}(\rho_{12}\operatorname{div}\mathbf{u}+\rho_{22}\operatorname{div}\mathbf{U})-\zeta\frac{\partial}{\partial t}\operatorname{div}(\mathbf{u}-\mathbf{U}),$$

$$G\nabla^2\operatorname{rot}\mathbf{u} = \frac{\partial^2}{\partial t^2}(\rho_{11}\operatorname{rot}\mathbf{u}+\rho_{12}\operatorname{rot}\mathbf{U})+\zeta\frac{\partial}{\partial t}\operatorname{rot}(\mathbf{u}-\mathbf{U}),$$

$$0 = \frac{\partial^2}{\partial t^2}(\rho_{12}\operatorname{rot}\mathbf{u}+\rho_{22}\operatorname{rot}\mathbf{U})-\zeta\frac{\partial}{\partial t}\operatorname{rot}(\mathbf{u}-\mathbf{U}).$$

In the latter set of equations $\mathbf{u}^T=\{u,0,w\}$ and $\mathbf{U}^T=\{U,0,W\}$ are the displacement vectors of the skeleton and the pore fluid, respectively; G, A, Q and R – elastic moduli of the medium, $(P=2G+A)$; $\rho_{11},\rho_{12},\rho_{22}$ – the mass coefficients; ζ – the damping parameter; t denotes time and ∇^2 – the Laplace operator.

The stress-strain relations for Biot's medium are defined by the equations:

$$\sigma_{ij} = 2Ge_{ij}+\delta_{ij}(A\operatorname{div}\mathbf{u}+Q\operatorname{div}\mathbf{U}), \quad (2)$$

$$s = Q\operatorname{div}\mathbf{u}+R\operatorname{div}\mathbf{U},$$

with the components of the skeleton strain tensor e_{ij} given by

$$e_{ij}=\frac{1}{2}(u_{i,j}+u_{j,i}). \quad (3)$$

In equations (2) σ_{ij} denotes the stress tensor in the skeleton, s the stress (tension) in the pore fluid, δ_{ij} the Kronecker symbol, i and j assume the values 1, 2, 3.

The equations of motion (1) should be supplemented by the boundary conditions. At the free surface $z = 0$ they take the form:

$$\begin{aligned} \sigma_{zz}(x,0,t) &= -q_{zz}(x)\exp(i\omega t), \\ \sigma_{xz}(x,0,t) &= -q_{xz}(x)\exp(i\omega t), \\ s(x,0,t) &= -q_s(x)\exp(i\omega t). \end{aligned} \tag{4}$$

In the above relations $q_{zz}(x)$, $q_{xz}(x)$ and $q_s(x)$ are the amplitudes of the exciting tractions applied at the surface $z = 0$.

At the artificial boundaries enclosing the finite rectangular region $ABCD$ (see Fig. 1) approximate absorbing conditions are supposed to be satisfied. Since the major part of the energy radiating from the source of disturbances is transmitted by a surface wave (Ewing et al. 1957) it seems reasonable to assume on the vertical planes $x = \pm L$ the conditions constructed specially for absorbing Rayleigh-type waves. In turn, at the horizontal boundary $z = h$ it is difficult to estimate the wave pattern approximately – it is possible only at relatively large distances from the source of disturbances. For this reason, we assume at the plane $z = h$ so-called standard viscous boundary conditions, i.e. those which ensure approximate absorption of the plane body waves. According to the above statement, we write:

– at the vertical boundaries $x = \pm L$

$$\begin{aligned} \sigma_{xx} &= -\lambda_1^R \frac{\partial u}{\partial t}, \\ s &= -\lambda_2^R \frac{\partial U}{\partial t}, \\ \sigma_{xz} &= -\lambda_3^R \frac{\partial w}{\partial t}; \end{aligned} \tag{5}$$

– at the horizontal boundary $x = h$

$$\begin{aligned} \sigma_{zz} &= -\lambda_1 \frac{\partial w}{\partial t}, \\ s &= -\lambda_2 \frac{\partial W}{\partial t}, \\ \sigma_{xz} &= -\lambda_3 \frac{\partial u}{\partial t}. \end{aligned} \tag{6}$$

Quantities λ_1^R, λ_2^R and λ_3^R are the parameters of the viscous dashpots which can perfectly absorb Rayleigh-type surface waves, and λ_1, λ_2 and λ_3 denote the dashpot parameters absorbing plane body waves arriving at the plane viscous boundary. It follows from the constitutive relations (2) that, in a general case, stresses in either component of the fluid-filled medium are coupled to each other through displacement

fields of both the skeleton and the pore water. In a particular case of variations harmonic in time, this coupling can be expressed by means of three factors, being complex numbers, which relate displacement vectors **u** and **U** to each other. These complex coefficients may by easily determined from the set of equations (1) by writing it for time-harmonic oscillations and then equating its main determinant to zero (Staroszczyk 1992a, 1992b). Accordingly, owing to the coupling of the two phases of the medium, it is sufficient to write at the right-hand sides of the first and the second equations of (5) and (6) velocities of only one component of the medium – either the skeleton or the pore fluid.

The proper evaluation of the viscous dashpot parameters is of key significance for the accuracy of the method discussed. In the case of surface waves the parameters λ_1^R, λ_2^R and λ_3^R can be determined exactly, because the stresses and velocities of the porous medium at the vertical boundary can be described explicitly as a function of depth from the free surface of the half-space. On the contrary, parameters λ_1, λ_2 and λ_3 can be evaluated only approximately. For example, by solving a problem of reflection of plane body waves at the plane viscous boundary. For an arbitrary angle of incidence and dashpot parameters λ_j a ratio between the energy transmitted by the reflected waves and that transmitted by the incident waves is evaluated. Then, such values of λ_1, λ_2 and λ_3 are sought, for which the energy ratio averaged over the whole range of possible angles of incidence (i.e. within the range $[0, \pi/2]$) reaches its minimum. The details of such an analysis can be found in the above-quoted paper (Staroszczyk 1992a). For purposes of the present investigation we only mention that the best absorbing ability of the viscous boundary occurs for values λ_j very close to those ensuring perfect absorption of waves arriving normally to the boundary. This means that to determine parameters λ_1, λ_2 and λ_3 it is sufficient to solve the one-dimensional wave propagation problem and the dashpot parameters obtained in such a way have been used in numerical calculations, the results of which are presented in section 4 of the present paper.

3. Discrete Solution of the Problem

The boundary-value problem, defined by equation (1) and (4) to (6), is solved in an approximate way by the use of the displacement-based finite element method. The rectangular, continuous domain $ABCD$ (see Fig. 1) is replaced by an assemblage of rectangular finite elements. A typical, four-node element is shown in Fig. 2.

In the plain strain conditions there are, in general, four non-zero components of the displacement vectors **u** and **U**. Let us denote by **f** the vector listing these components:

$$\mathbf{f}^T = \{u, w, U, W\}. \tag{7}$$

Since there are 4 degrees of freedom per node, the element nodal displacement vector $\boldsymbol{\delta}^e$ contains 16 components:

$$\boldsymbol{\delta}^e = \{\boldsymbol{\delta}_i, \boldsymbol{\delta}_j, \boldsymbol{\delta}_k, \boldsymbol{\delta}_l, \}^T \tag{8}$$

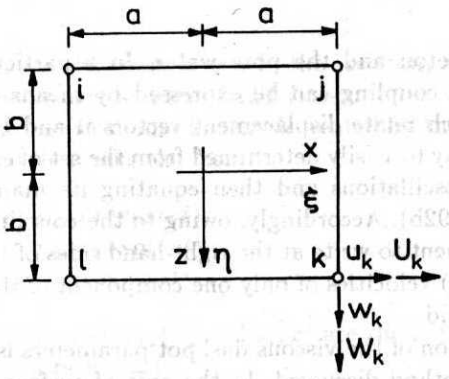

Fig. 2. Rectangular finite element and local coordinate systems

with $\delta_r^T = \{u_r, w_r, U_r, W_r\}$ $(r = i, j, k, l)$ being the displacement vector corresponding to node r. We assume the linear variation of the displacements u, w, U and W within the finite element, i.e. the following shape functions are considered (Zienkiewicz 1977):

$$N_r = \frac{1}{4}(1 + \xi_r \xi)(1 + \eta_r \eta), \quad r = i, j, k, l, \tag{9}$$

where, for convenience, we have introduced dimensionless coordinates defined by

$$\xi = x/a, \quad \eta = z/b, \tag{10}$$

and $(\xi_r, \eta_r) = (\pm 1, \pm 1)$ are the coordinates of the finite element nodes in the local coordinate system $0\xi\eta$. Using the shape functions (9) we relate the displacements $\mathbf{f}$ within the element to the nodal displacements δ^e by means of the formula:

$$\mathbf{f} = \mathbf{N}\delta^e, \tag{11}$$

where the interpolation functions matrix $\mathbf{N}$ has the form

$$\mathbf{N} = [N_i\mathbf{I}, N_j\mathbf{I}, N_k\mathbf{I}, N_l\mathbf{I}] \tag{12}$$

and $\mathbf{I}$ is the identity matrix (4×4). The non-zero strains (3) related to the displacement vector $\mathbf{f}$ are:

$$\mathbf{e}^T = \{e_{xx}, e_{zz}, \gamma_{xz}, \epsilon\}, \tag{13}$$

where $\gamma_{xz} = 2e_{xz}$, and $\epsilon = \operatorname{div}\mathbf{U}$ is the dilatation of the pore fluid. Employing relations (3) and (11) we express strains (13) in terms of the element nodal displacements δ^e as follows:

$$\mathbf{e} = \mathbf{B}\delta^e, \tag{14}$$

where the strain-displacement transformation matrix $\mathbf{B}$ is defined by

$$\mathbf{B} = [\mathbf{B}_i, \mathbf{B}_j, \mathbf{B}_k, \mathbf{B}_l] \tag{15}$$

and consists of four square submatrices of the form:

$$\mathbf{B} = \frac{1}{4ab}\begin{bmatrix} b_1^r & 0 & 0 & 0 \\ 0 & b_2^r & 0 & 0 \\ b_2^r & b_1^r & 0 & 0 \\ 0 & 0 & b_1^r & b_2^r \end{bmatrix}, \quad r = i, j, k, l, \tag{16}$$

with $b_1^r = \xi_r(b + \eta_r z)$ and $b_2^r = \eta_r(a + \xi_r x)$. We list the stresses corresponding to the strains $\mathbf{e}$ in the vector $\boldsymbol{\sigma}$:

$$\boldsymbol{\sigma}^T = \{\sigma_{xx}, \sigma_{zz}, \sigma_{xz}, s\}. \tag{17}$$

The constitutive relations (2) may now by written in the form:

$$\boldsymbol{\sigma} = \mathbf{De}, \tag{18}$$

where $\mathbf{D}$ is the elasticity matrix of Biot's medium in the plane strain conditions and has the form:

$$\mathbf{D} = \begin{bmatrix} P & A & 0 & Q \\ A & P & 0 & Q \\ 0 & 0 & G & 0 \\ Q & Q & 0 & R \end{bmatrix}. \tag{19}$$

By applying the principle of virtual work we derive the following system of equilibrium equations for the finite element:

$$\mathbf{k}^e\delta^e + \mathbf{c}^e\frac{\partial}{\partial t}\delta^e + \mathbf{m}^e\frac{\partial^2}{\partial t^2}\delta^e = \mathbf{F}^e, \tag{20}$$

where $\mathbf{F}^e$ denotes the vector of nodal forces corresponding to the element degrees of freedom. The element stiffness matrix $\mathbf{k}^e$ is defined by the formula:

$$\mathbf{k}^e = \int_{-a}^{a}\int_{-b}^{b} \mathbf{B}^T\mathbf{DB}\,dx\,dz, \tag{21}$$

and consists of sixteen (4×4) submatrices:

$$\mathbf{k}^e = \begin{bmatrix} \mathbf{k}_{ii} & \mathbf{k}_{ij} & \mathbf{k}_{ik} & \mathbf{k}_{il} \\ \mathbf{k}_{ji} & \mathbf{k}_{jj} & \mathbf{k}_{jk} & \mathbf{k}_{jl} \\ \mathbf{k}_{ki} & \mathbf{k}_{kj} & \mathbf{k}_{kk} & \mathbf{k}_{kl} \\ \mathbf{k}_{li} & \mathbf{k}_{lj} & \mathbf{k}_{lk} & \mathbf{k}_{ll} \end{bmatrix}. \tag{22}$$

Each of the submatrices $\mathbf{k}_{rs}^e$ has the form:

$$\mathbf{k}_{rs}^e = \begin{bmatrix} PI_{11}^{rs} + GI_{22}^{rs} & AI_{12}^{rs} + GI_{21}^{rs} & QI_{11}^{rs} & QI_{12}^{rs} \\ AI_{21}^{rs} + GI_{12}^{rs} & PI_{22}^{rs} + GI_{11}^{rs} & QI_{21}^{rs} & QI_{22}^{rs} \\ QI_{11}^{rs} & QI_{12}^{rs} & RI_{11}^{rs} & RI_{12}^{rs} \\ QI_{21}^{rs} & QI_{22}^{rs} & RI_{21}^{rs} & RI_{22}^{rs} \end{bmatrix}, \tag{23}$$

where:

$$\begin{aligned} I_{11}^{rs} &= \frac{\xi_r \xi_s}{4}\frac{b}{a}\left(1+\frac{1}{3}\eta_r\eta_s\right), \quad I_{12}^{rs} = \frac{\xi_r \eta_s}{4}, \\ I_{21}^{rs} &= \frac{\eta_r \xi_s}{4}, \quad I_{22}^{rs} = \frac{\eta_r \eta_s}{4}\frac{a}{b}\left(1+\frac{1}{3}\xi_r\xi_s\right), \quad r,s = i,j,k,l. \end{aligned} \tag{24}$$

The element damping matrix $\mathbf{c}^e$ is given by the relation:

$$\mathbf{c}^e = \zeta \int_{-a}^{a}\int_{-b}^{b} \mathbf{N}^T \mathbf{E} \mathbf{N} dx dz, \tag{25}$$

with

$$\mathbf{E} = \begin{bmatrix} 1 & 0 & -1 & 0 \\ 0 & 1 & 0 & -1 \\ -1 & 0 & 1 & 0 \\ 0 & -1 & 0 & 1 \end{bmatrix}. \tag{26}$$

Like the stiffness matrix $\mathbf{k}^e$, the matrix $\mathbf{c}^e$ is also composed of sixteen (4×4) submatrices, determined by the formula:

$$\mathbf{c}_{rs}^e = \zeta I_0^{rs} \mathbf{E}, \quad r,s = i,j,k,l, \tag{27}$$

with

$$I_0^{rs} = \frac{ab}{4}\left(1+\frac{1}{3}\xi_r\xi_s\right)\left(1+\frac{1}{3}\eta_r\eta_s\right). \tag{28}$$

Finally, the element mass matrix $\mathbf{m}^e$ is defined by means of:

$$\mathbf{m}^e = \int_{-a}^{a}\int_{-b}^{b} \mathbf{N}^T \rho \mathbf{N} dx dz, \tag{29}$$

where the matrix ρ appears:

$$\rho = \begin{bmatrix} \rho_{11} & 0 & \rho_{12} & 0 \\ 0 & \rho_{11} & 0 & \rho_{12} \\ \rho_{12} & 0 & \rho_{22} & 0 \\ 0 & \rho_{12} & 0 & \rho_{22} \end{bmatrix}. \tag{30}$$

Also, the matrix $\mathbf{m}^e$ consists of (4×4) submatrices of the form:

$$\mathbf{m}_{rs}^e = I_0^{rs} \rho, \quad r,s = i,j,k,l. \tag{31}$$

Performing for the whole structure considered the direct addition of the element stiffness, damping and mass matrices, and keeping in mind that time harmonic variations are analysed, we arrive at the final set of equations corresponding to the problem under discussion:

$$\overline{\mathbf{K}}\boldsymbol{\delta} = \mathbf{F}, \tag{32}$$

with the complex stiffness matrix $\overline{\mathbf{K}}$ of the form:

$$\overline{\mathbf{K}} = \mathbf{K} + i\omega\mathbf{C} - \omega^2\mathbf{M}. \tag{33}$$

In equations $\boldsymbol{\delta}$ and $\mathbf{F}$ are the structure displacement and nodal point load vectors; $\mathbf{K}, \mathbf{C}$ and $\mathbf{M}$ are the structure stiffness, damping and mass matrices, respectively.

Before solving the set of equations (32), the stiffness matrix $\overline{\mathbf{K}}$ has to be modified so as to satisfy the boundary conditions of the problem. Imposition of absorbing conditions (5) and (6) results in the adding of the appropriate stiffness parameters to the relevant diagonal elements of $\overline{\mathbf{K}}$. The stiffness parameters mentioned are evaluated by integrating the functions describing the distribution of the viscous dashpots over the sides of finite elements adjacent to the imaginary boundaries. In the case of the nodal point displacement conditions being specified (for instance at the plane of symmetry of the problem) the so-called penalty method has been employed (Bathe 1982). This method has the advantage of only the diagonal elements of the structure stiffness matrix being modified, which leads to a numerically stable solution of the resultant set of equations (32).

4. Numerical Examples

On the basis of the discrete method presented, a numerical model of the problem discussed has been constructed. In order to decrease a number of nodal points of the discrete system we have confined consideration to a problem symmetric with respect to z-axis – the model corresponding to the latter is shown in Fig. 3. It consists of a non-uniform mesh of rectangular finite elements. The mesh spacings change in both horizontal and vertical directions – they increase gradually with growing distance from the zone of excitation. The model has had 20 nodes along x-axis and 15 nodes along z-axis (266 finite elements, 1200 system degrees of freedom). In order to ensure acceptable accuracy of the discrete model the maximum mesh sizes should not exceed certain values, defined by the lengths of waves propagating in the porous medium. The numerical tests have shown that for obtaining satisfactory results it is sufficient to maintain the maximum finite element sides in limits of about 1/10 to 1/8 of the wavelength of the Rayleigh surface wave L_R. An another factor that strongly influences the accuracy of the numerical results is the distance from the source of disturbances to the artificial boundaries, as the latter absorb arriving wave energy imperfectly. It has been found that this distance should not be less than about 3/4 of the surface wave length. In the model used in computations, the above-mentioned distance, defined by the sides of the rectangle $ABEO$ in Fig. 3, has been assumed to be equal to the one length of the surface wave, i.e. $h = L = L_R$.

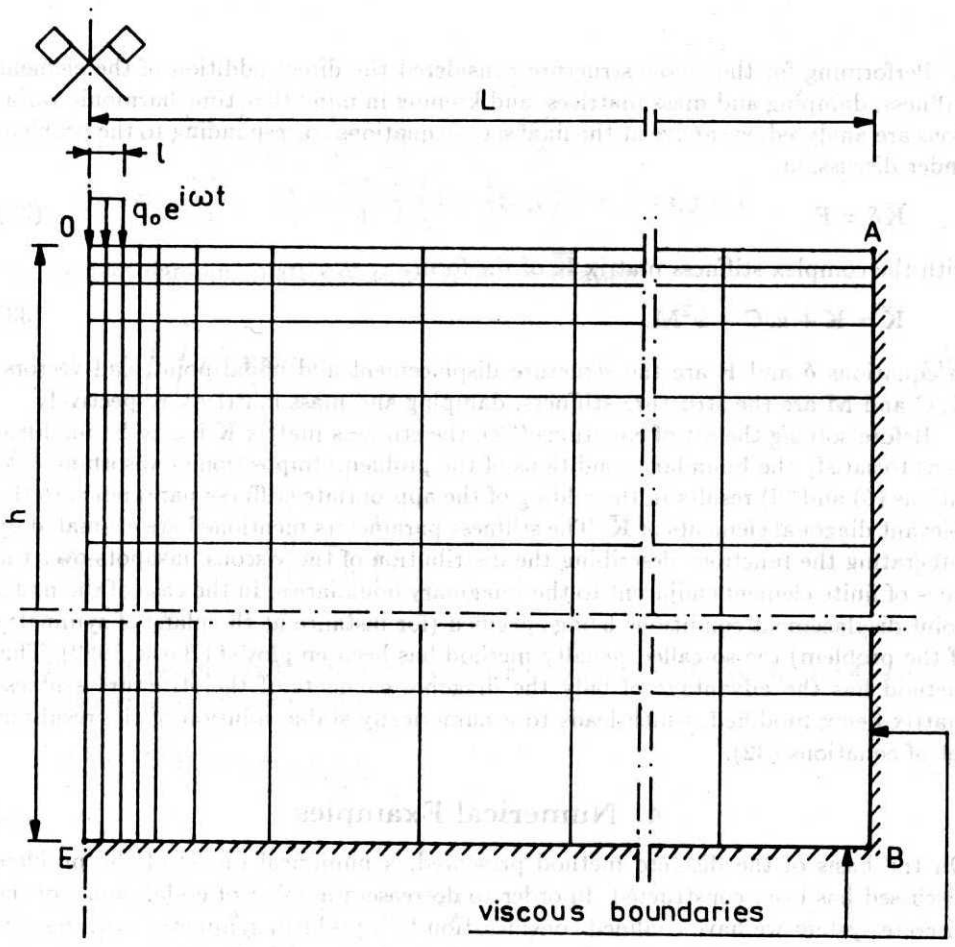

Fig. 3. Discrete model of the problem

The numerical calculations have been carried out for material parameters pertaining to a coarse sand filled with water:

$$G = 3.75 \times 10^8\,\text{Pa}, \quad A = 2.82 \times 10^9\,\text{Pa},$$
$$Q = 1.38 \times 10^9\,\text{Pa}, \quad R = 9.2 \times 10^8\,\text{Pa},$$
$$\rho_{11} = 1590\,\text{kg/m}^3, \quad \rho_{22} = 400\,\text{kg/m}^3,$$
$$\rho_{12} = 0, \quad \zeta = 1.57 \times 10^5\,\text{Ns/m}^4.$$

These data correspond to the coarse sand of a real mass density of the skeleton $\rho_s = 2650$ kg/m^3, a porosity $n = 0.4$ and a filtration coefficient $k_f = 0.01$ m/s. As an example, we present the numerical results obtained for a particular case with the surface load in the form of a step function of constant pressure q_0, applied to the

porous skeleton over a segment $-l \leq x \leq l$ normally to the free surface $z = 0$. The boundary conditions (4) have now the form:

$$\begin{aligned} \sigma_{zz}(x,0,t) &= \begin{cases} -q_0 \exp(i\omega t), & |x| \leq l, \\ 0, & |x| > l, \end{cases} \\ \sigma_{xz}(x,0,t) &= s(x,0,t) = 0, \qquad |x| < \infty. \end{aligned} \tag{34}$$

For a given exciting load we calculate the components of the skeleton and the pore water displacement vectors u, w, U and W. For convenience we express them in the dimensionless form:

$$\begin{aligned} \overline{u} &= |\overline{u}| \exp[i(\omega t + \delta_u)] = \tfrac{\pi G k_r u}{2q_0}, \\ \overline{w} &= |\overline{w}| \exp[i(\omega t + \delta_w)] = \tfrac{\pi G k_r w}{2q_0}, \end{aligned} \tag{35}$$

where $|\overline{u}|$ and $|\overline{w}|$ are the complex moduli (amplitudes) of the dimensionless horizontal $\overline{u}$ and vertical $\overline{w}$ skeleton displacements, while δ_u and δ_w are the complex arguments (phase angles) of these displacements. Expressions similar to the latter can be written for the pore water displacement wector components U and W. The parameter k_r, appearing in (35), denotes the wave number of the distorsional wave propagating in the unbounded two-phase medium.

In Figure 4 we plot the amplitudes of the dimensionless vertical displacements (35) of the skeleton and the pore water in the vicinity of the zone of excitation for the case of angular frequency $\omega = 4.341\ \mathrm{s}^{-1}$ and $l = 10$ m (which correspond to the dimensionless frequency $k_r l = 0.1$). The results computed by means of the discrete method are compared with those obtained analytically (Staroszczyk 1992b). It is seen that a good agreement between the results of the two methods has been reached. The largest relative differences occur near the region of external load application and for frequency considered they are equal to about 7 per cent for the skeleton and about 9 per cent for the pore water (for $x = 0, z = l$). At points more distant from the source of disturbances the relative discrepancies are smaller, e.g. for $|x|$ or $z \gtrsim 5l$ they do not exceed 4 per cent for both phases of the porous solid.

In engineering practice we are most often interested only in displacements of the free surface of the half-space. Some of the numerical results concerning the free surface vertical displacement amplitudes at different dimensionless frequencies $k_r l$ are listed in Table 1. One may observe that at higher frequencies an average accuracy of the results slightly improves. At the frequency $k_r l = 0.1$ the maximum discrepancies between the discrete and the analytical results equal 5.8 per cent for the skeleton and 8.1 per cent for the pore fluid, while at $k_r l = 1.0$ these values are equal to 5.7 per cent for both the components of the medium. At greater distances ($|x| = 5l$) the results differ by not more than 3.7 per cent for both the skeleton and the pore water.

In order to investigate the influence of the frequency of oscillations on the accuracy of the method, some calculations have been performed for a wide range of dimensionless frequency parameter $0.1 \leq k_r l \leq 1.5$. The discrete results obtained against the

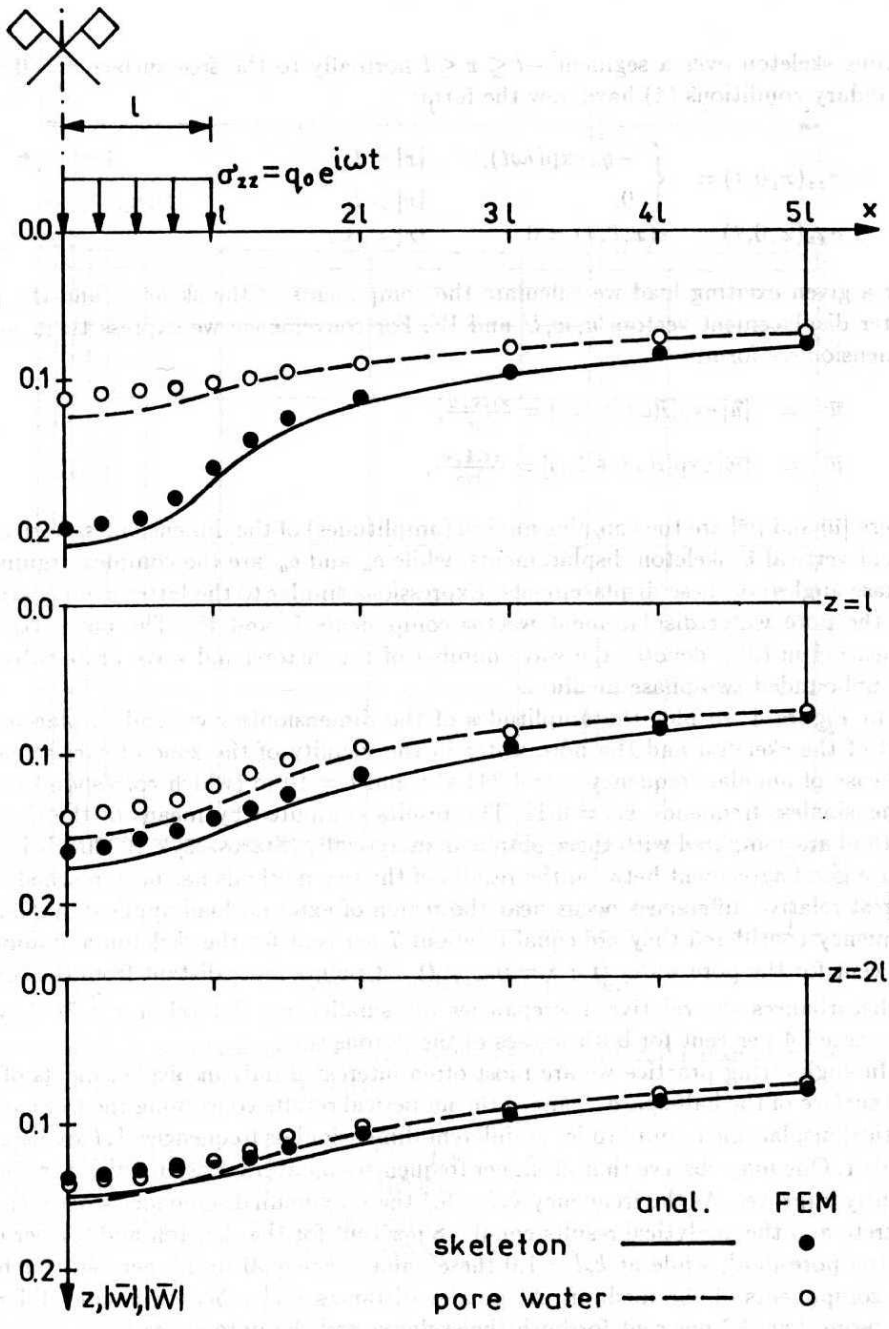

Fig. 4. Dimensionless vertical displacement amplitudes – comparison of analytical and FEM results (coarse sand, $k_r l = 0.1$)

Table 1

Dimensionless vertical displacement amplitudes at the free surface – comparison of analytical and FEM results (coarse sand, $l = 10$ m)

$k_r l$	x/l	Skeleton		Pore water	
		Anal.	FEM	Anal.	FEM
0.1	0.0	0.2090	0.1968	0.1231	0.1131
	1.0	0.1683	0.1588	0.1081	0.1017
	2.0	0.1181	0.1124	0.0891	0.0898
	3.0	0.0986	0.0948	0.0812	0.0822
	4.0	0.0869	0.0842	0.0758	0.0736
	5.0	0.0791	0.0767	0.0719	0.0704
0.5	0.0	0.6265	0.6130	0.3659	0.3801
	1.0	0.4424	0.4253	0.3005	0.2922
	2.0	0.3094	0.2967	0.2640	0.2543
	3.0	0.2819	0.2653	0.2606	0.2510
	4.0	0.2730	0.2626	0.2609	0.2501
	5.0	0.2680	0.2609	0.2592	0.2495
1.0	0.0	0.9076	0.8983	0.5597	0.5915
	1.0	0.5250	0.5212	0.4242	0.4215
	2.0	0.4628	0.4309	0.4391	0.4183
	3.0	0.4527	0.4271	0.4340	0.4144
	4.0	0.4143	0.4030	0.3907	0.3906
	5.0	0.3467	0.3440	0.3133	0.3131

analytical ones are plotted in Fig. 5. Since, as a rule, the largest discrepancies between the results of both the methods occur in the neighbourhood of the excitation zone, we have confined our attention to the vertical displacements at the origin of the coordinate system. The plots exhibit the small differences between the discrete and the analytical results within the whole frequency range. The mean square relative deviations between the results of the two methods are for both the components of the medium almost equal to each other: 3.4 per cent for the skeleton and 3.6 per cent for the pore fluid. Slightly larger discrepancies are observed at low frequencies ($k_r l \tilde{<} 0.2$), while at higher ones ($k_r l > 0.5$) the accuracy of the discrete method increases.

5. Final Remarks

In the paper we have investigated the applicability of the earlier formulated (Staroszczyk 1992a) approximate absorbing boundary conditions for Biot's media in solving harmonic in time, semi-infinite problems. To this aim, Lamb's problem has been solved by the use of the finite element method. On the basis of the discrete model constructed, some numerical computations for a water-filled coarse sand have been performed. The numerical results obtained reveal a good agreement with those evaluated analytically within a wide range of frequencies. The displacement amplitudes

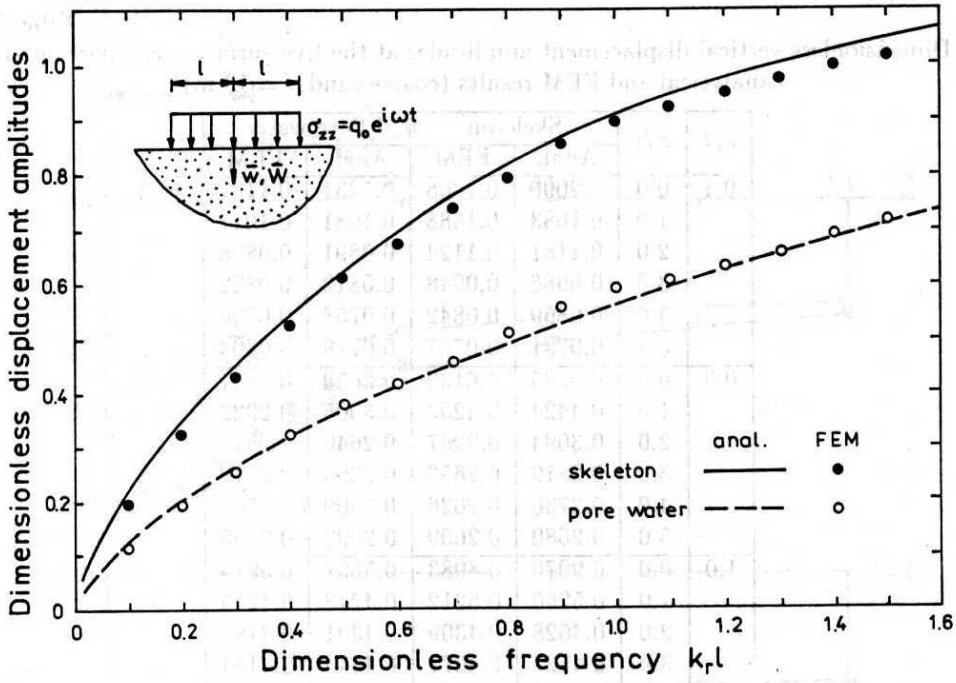

Fig. 5. Dimensionless vertical displacement amplitudes at the origin of the coordinate system at different frequencies – comparison of analytical and FEM results (coarse sand, $l = 10$ m)

calculated by means of the two methods differ at most by 7 per cent for the porous skeleton and 9 per cent for the pore water directly near the excited zone, and not more than about 4 per cent for both the components of the medium at points distant from the source of disturbances. It has been found that in order to ensure satisfactory accuracy of the discrete results the maximum finite element dimensions ought not to exceed 1/10 to 1/8 of the wavelength of the surface wave. The number of discrete points over the wavelength should be greater as the frequency of oscillations decreases. The artificial absorbing boundaries should be situated at distances of about one or more wavelength of the Rayleigh wave from the excitation zone. One should note that, due to the approximate character of the absorbing boundary conditions applied, it is difficult to achieve a better accuracy of the method by increasing the number of nodes of the discrete system. But even so, the results obtained allow us to expect that the discrete approach presented in this investigation will be useful in the analysis of more complex problems, which cannot be solved otherwise than by the use of discrete methods.

References

Bathe K.-J. (1982), *Finite element procedures in engineering analysis*, Prentice-Hall, Englewood Cliffs, New Jersey.

Biot M.A. (1956), *Theory of propagation of elastic waves in a fluid-saturated porous solid*, J. Acoust. Soc. Am., 28, pp. 168-191.

Ewing W.M., Jardetzky W.S., Press F. (1957), *Elastic waves in layered media*, McGraw-Hill Book Company, New York.

Filipkowski J., Sienkiewicz Z. (1988), *Numerical solution of a steady-state wave field in two-dimensional viscoelastic media*, Mechanika i Komputer, 7, pp. 71-86, (in Polish).

Lysmer J., Kuhlemeyer R.L. (1969), *Finite dynamic model for infinite media*, J. Engng. Mech. Div., Proc. ASCE, 95, 4, pp. 859-877.

Staroszczyk R. (1992a), *Absorbing boundary conditions for waves in Biot's media*, Hydrotechnical Transactions, Vol. 55, pp. 169-189.

Staroszczyk R. (1992b), *Steady-state plane Lamb's problem for a fluid-saturated poroelastic medium*, Archives of Mechanics, 44, 5, pp. 499-512.

Zienkiewicz O.C. (1977), *The finite element method*, McGraw-Hill, London.

Summary

The paper deals with Lamb's time harmonic plane problem for a fluid-filled poroelastic medium. The analysis is carried out within the framework of Biot's dynamical theory of consolidation. The problem is solved in a discrete way by the use of the finite element method. In order to reduce considerations to a finite domain artificial boundaries are introduced. At these boundaries a system of infinitesimal viscous dashpots, the aim of which is to absorb incoming wave energy, is set up. Employing the discrete model of the problem some numerical calculations for a water-saturated coarse sand have been carried out. Comparison of the numerical results obtained against those evaluated analytically shows satisfactory accuracy of the discrete approach presented.

Rozwiązanie ustalonego płaskiego zagadnienia Lamba dla ośrodka Biota metodą elementów skończonych

Streszczenie

W pracy rozważa się harmonicznie zmienne w czasie płaskie zagadnienia Lamba dla sprężystego ośrodka porowatego wypełnionego cieczą. Dyskusję przeprowadzono w oparciu o dynamiczną teorię konsolidacji Biota. Zadanie rozwiązano w sposób dyskretny, stosując metodę elementów skończonych. W celu ograniczenia rozważań do obszaru o skończonych wymiarach wprowadzono sztuczne brzegi. Na brzegach tych umieszczono system zastępczych tłumików lepkich, których zadaniem jest pochłanianie energii fal padających na brzeg. Wykorzystując model dyskretny zagadnienia wykonano obliczenia numeryczne dla nawodnionego piasku grubego. Porównanie

otrzymanych wyników numerycznych z rezultatami uzyskanymi w sposób analityczny wskazuje na zadowalającą dokładność zaprezentowanego podejścia dyskretnego.